Ca^{2+}-activated K^+ channel inhibition by reactive oxygen species

MARCO A. SOTO,[1,2,3] CARLOS GONZÁLEZ,[1,2] EDUARDO LISSI,[3]
CECILIA VERGARA,[1,2] AND RAMÓN LATORRE[1,2]
[1]*Centro de Estudios Científicos, Valdivia;* [2]*Facultad de Ciencias, Universidad de Chile, Santiago; and* [3]*Facultad de Química y Biología, Universidad de Santiago, Santiago, Chile*

Soto, Marco A., Carlos González, Eduardo Lissi, Cecilia Vergara, and Ramón Latorre. Ca^{2+}-activated K^+ channel inhibition by reactive oxygen species. *Am J Physiol Cell Physiol* 282: C461–C471, 2002. First published September 21, 2001; 10.1152/ajpcell.00167.2001.—We studied the effect of H_2O_2 on the gating behavior of large-conductance Ca^{2+}-sensitive voltage-dependent K^+ ($K_{V,Ca}$) channels. We recorded potassium currents from single skeletal muscle channels incorporated into bilayers or using macropatches of *Xenopus laevis* oocytes membranes expressing the human *Slowpoke* (h*Slo*) α-subunit. Exposure of the intracellular side of $K_{V,Ca}$ channels to H_2O_2 (4–23 mM) leads to a time-dependent decrease of the open probability (P_o) without affecting the unitary conductance. H_2O_2 did not affect channel activity when added to the extracellular side. These results provide evidence for an intracellular site(s) of H_2O_2 action. Desferrioxamine (60 μM) and cysteine (1 mM) completely inhibited the effect of H_2O_2, indicating that the decrease in P_o was mediated by hydroxyl radicals. The reducing agent dithiothreitol (DTT) could not fully reverse the effect of H_2O_2. However, DTT did completely reverse the decrease in P_o induced by the oxidizing agent 5,5′-dithio-bis-(2-nitrobenzoic acid). The incomplete recovery of $K_{V,Ca}$ channel activity promoted by DTT suggests that H_2O_2 treatment must be modifying other amino acid residues, e.g., as methionine or tryptophan, besides cysteine. Noise analysis of macroscopic currents in *Xenopus* oocytes expressing h*Slo* channels showed that H_2O_2 induced a decrease in current mediated by a decrease both in the number of active channels and P_o.

$K_{V,Ca}$ channels; H_2O_2

MOLECULAR OXYGEN OCCUPIES an essential role in many of the metabolic processes associated with aerobic existence. Hydrogen peroxide (H_2O_2), superoxide radical anion (O_2^-), singlet oxygen ($^1O_2$), and hydroxyl radical (·OH) are produced by intracellular metabolism from a variety of cytosolic enzyme systems. NADPH oxidase and nitric oxide synthase (NOS) family contributes to oxidative stress due to the generation of free radicals. Free radicals production is regulated by an enzymatic defensive system (superoxide dismutase, catalase, glutathione peroxidase) and a nonenzymatic system that includes pyruvate, ascorbate, carotenes, and glutathione. The equilibrium between free radical production and antioxidant defenses determines the degree of oxidative stress (13).

The levels of reactive oxygen species (ROS) are enhanced during inflammation, radiation exposure, endotoxic shock, and ischemia-reperfusion. The pathologies that have been attributed to ROS-induced cell dysfunction include skeletal muscle injury (27, 30) and myocardial damage during ischemia and reperfusion. In skeletal muscle, exercise increases the rate of ROS production. This increase is associated with increased levels of lipid peroxidation and peroxidation products, low catalase concentrations, and the presence of high levels of myoglobin acting as a catalyst for the formation of oxidants (8, 27). Kourie (19) reviews the effects of ROS when interacting with ion transport systems.

Calcium- and voltage-sensitive channels of large unitary conductance ($K_{V,Ca}$) are distributed in different cells and tissues, where they modulate many cellular processes (20, 21). Because cytosolic Ca^{2+} activates $K_{V,Ca}$ channels, they play an important role in coupling chemical to electric signaling. $K_{V,Ca}$ channels are present abundantly in virtually all types of smooth muscle cells, where they control the resting tone (1, 17, 24). $K_{V,Ca}$ channels are also redox modulated (10, 38, 39). For instance, oxidizing agents such as H_2O_2 promote channel inhibition, and the reducing agent dithiothreitol (DTT) augments channel activity (10). The effect of H_2O_2 on the $K_{V,Ca}$ channel was studied by DiChiara and Reinhart (10). They reported that h*Slo* currents were downmodulated by the oxidizing agent with a right shift of the probability of opening (P_o) vs. voltage curves and a decrease in the single-channel P_o. In the present study, we examined the mode of action of H_2O_2 in detail, with the aim of finding a mechanistic explanation for its deleterious effects on $K_{V,Ca}$ channels. We found that *1*) the targets of H_2O_2 action are located in the intracellular aspect of the $K_{V,Ca}$ channel; and *2*) the H_2O_2 effect on the $K_{V,Ca}$ channel activity is mediated by ·OH. The general conclusion is that redox modulation most probably involves a disulfide/thiol exchange of thiol groups of some of the numerous

Address for reprint requests and other correspondence: M. A. Soto Arriaza, Centro de Estudios Científicos (CECS), Av. Arturo Prat 514, Valdivia, Chile (E-mail: marcos@cecs.cl).

The costs of publication of this article were defrayed in part by the payment of page charges. The article must therefore be hereby marked "*advertisement*" in accordance with 18 U.S.C. Section 1734 solely to indicate this fact.

cysteines present in the carboxy terminus of the human *Slowpoke* (h*Slo*) protein.

METHODS

Planar lipid bilayers and single channel recordings. Lipid bilayers were made from an 8:1 mixture of 1-palmitoyl, 2-oleoyl phosphatidylethanolamine (POPE) and 1-palmitoyl, 2-oleoyl phosphatidylcholine (POPC) in decane (13 mg lipid/ml). This lipid solution was applied across a small hole (0.2–0.3 mm in diameter) made in the wall of a Delrin cup separating two chambers of 3.5 ml *cis*- and 0.35 ml *trans*-containing symmetric salt solutions of 150 mM KCl, 10 mM 3-[*N*-morpholino]propanesulfonic acid K^+ salt , pH 7, $[Ca^{2+}] \cong 5$ μM. Bilayer formation was followed by measuring membrane capacitance. Bilayer capacitance was measured at the end of each experiment to determine possible changes in bilayer area and/or thickness. Rat skeletal muscle was used to prepare tubule T membrane vesicles containing $K_{V,Ca}$ channels as previously described (22). Membrane vesicles were added very close to the bilayer. Because depolarizing voltages and cytoplasmic Ca^{2+} activate $K_{V,Ca}$ channels, the internal side of the membrane was defined according to the voltage and Ca^{2+} dependence of the channel. H_2O_2 from a concentrated stock solution was added to the indicated concentrations. The solutions were stirred for 30 s, and single-channel current records (3–60 min) were obtained at a constant applied potential of +60 mV unless otherwise stated.

Comparisons between current records obtained in the different experimental conditions tested were taken in the same single-channel membrane. Only membranes with a stable P_o were used.

Data acquisition and analysis. The current across the bilayer was measured with a low-noise current-to-voltage converter (6) connected to the solution through agar bridges made with 1 M KCl. Continuous 3- to 60-min single-channel current records were taped on a video recorder. For analysis, the current was filtered at 400 Hz with an eight-pole Bessel low-pass active filter and digitized at 500 μs/point. The electrophysiological convention was used, in which the external side of the channel was defined as zero potential. The experiments were conducted at room temperature (22 ± 2°C).

Open and closed events were identified using a discriminator located at 50% of the open-channel current. Dwell-time histograms were logarithmically binned and fitted to a sum of exponential probability functions with pClamp 6.0 software (Axon Instrument). Closed dwell-time histograms were fitted to the sum of two exponential functions.

P_o was measured as a function of time after H_2O_2 addition and $[H_2O_2]$. For single-channel membranes, P_o was obtained as the time spent in the fully open current level divided by the total time of the record, usually 60 s. P_o values were calculated excluding channel closures lasting >200 ms as these events are due to ion channel blockage induced by the contaminant Ba^{2+} (9, 25).

Oocyte isolation and RNA injection. Ovarian lobes were surgically removed from adult female *X. laevis* (Nasco) and placed in 100-mm petri dishes containing OR-2 solution (in mM: 83 NaCl, 2.5 KCl, 1 $MgCl_2$, 5 HEPES; pH 7.6). To dissociate the oocytes, the lobes were incubated for 60 min at 18°C in OR-2 solution containing 1 mg/ml collagenase (GIBCO BRL). Dissociated oocytes were placed in ND-96 solution (100 mM NaCl, 2 mM KCl, 1.8 mM $CaCl_2$, 1 mM $MgCl_2$, 5 mM HEPES, and 50 μg/ml gentamicin, pH 7.4) and were injected with 50 nl of a solution of human myometrial cRNA of the h*Slo* channel α-subunit containing 100 ng/μl. Oocytes were kept at 18°C in an incubator and were used for the experiments 3–4 days after RNA injection.

Electrophysiology. Macroscopic currents were recorded in cell-attached macropatches and excised inside-out patches. Patch pipettes resistance were ~1 MΩ. Bath and pipettes contained (in mM): 110 KMES, 10 HEPES, 5 HEDTA (the affinity of HEDTA for iron is about 100-fold less compared with EDTA), pH 7.0, and the indicated Ca^{2+} concentrations. The acquisition and basic analysis of the data were performed with pClamp 6.0 software (Axon Instruments) driving a 12-bit analog interface card (Labmaster DMA, Scientific Solutions).

Variance analysis. A series of current traces were recorded after pulsing to a positive voltage from the holding potential. The average basal variance at the holding voltage was subtracted from the variance obtained during the test pulse. The subtracted variance (σ^2) was plotted vs. mean current [$I(t)$] and the data were fitted using (31)

$$\sigma^2 = iI(t) - I(t)^2/N \quad (1)$$

where i is the single-channel current amplitude and N the number of channels; i was obtained from the initial slope; N was obtained from the nonlinear curve-fitting analysis done using Microsoft Excel. The maximum open probability (P_o^{max}) was obtained according to the relation: $P_o^{max} = I_{max}/iN$, where I_{max} is the maximum mean current measured in the experiment.

Reagents. POPE and POPC in chloroform were purchased from Avanti Polar Lipids (Birmingham, AL). The 5,5′-dithiobis-(2-nitrobenzoic acid) (DTNB), DTT, and *n*-decane were purchased from Sigma (St. Louis, MO). The perhydrol 30% of hydrogen peroxide, chloroform, ethanol, and methanol were purchased from Merck Chemical.

RESULTS

Effect of H_2O_2 addition on the $K_{V,Ca}$ single channels. Fig. 1, *A* and *B*, shows single-channel current records in the absence (control) and presence of 23 mM H_2O_2 added to the external and internal side, respectively. This experiment shows that H_2O_2 does not affect the P_o when added to the external side; P_o value remains constant even after 30 min of H_2O_2 addition. On the other hand, when the internal side was exposed to the same $[H_2O_2]$, P_o decreased from 0.621 ± 0.032 to 0.081 ± 0.022 ($n = 5$) after just 3 min of addition (Fig. 1, *B* and *C*). However, the unitary conductance remained constant during the time experiments (see Fig. 1*B*, insets *a* and *b*). At this $[H_2O_2]$, channel P_o decreases to a very low value in a few seconds. It is surprising that H_2O_2, despite its large membrane permeability coefficient, is ineffective when applied to the external side. This is due to the fact that, in these experiments, H_2O_2 (23 mM) was added to an external compartment having a volume of 0.35 cm^3, and the internal compartment had a volume of 3.3 cm^3. Considering a H_2O_2 permeability coefficient of 10^{-4} cms^{-1} and a bilayer area of 3.14×10^{-4} cm^2, the maximum $[H_2O_2]$ that can be reached in the internal compartment is only about 2 mM, and the time to reach this concentration is >1,000 h. Even if this volume is restricted by the unstirred layers (~100 μm in thickness), the time needed to reach a concentration >4 mM (the smallest $[H_2O_2]$ tested; see Fig. 2*B*) would be several hours.

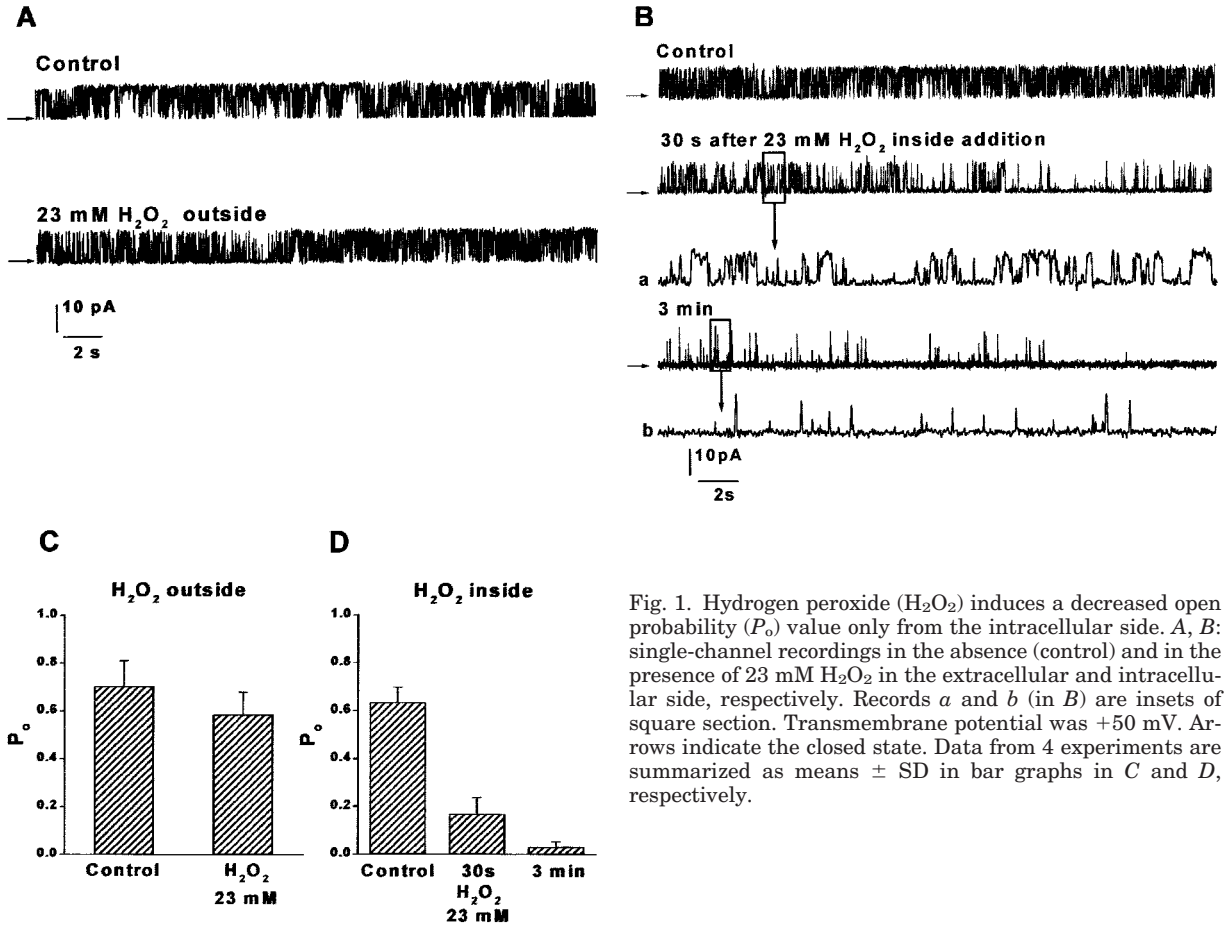

Fig. 1. Hydrogen peroxide (H_2O_2) induces a decreased open probability (P_o) value only from the intracellular side. *A*, *B*: single-channel recordings in the absence (control) and in the presence of 23 mM H_2O_2 in the extracellular and intracellular side, respectively. Records *a* and *b* (in *B*) are insets of square section. Transmembrane potential was +50 mV. Arrows indicate the closed state. Data from 4 experiments are summarized as means ± SD in bar graphs in *C* and *D*, respectively.

Figure 2*A* shows single-channel current records from a $K_{V,Ca}$ channel in the absence (control) and presence of 8 mM H_2O_2 added to the internal side. In this condition, the P_o decreased from 0.895 ± 0.041 (control, $t = 0$) to 0.051 ± 0.012 ($n = 5$) after 30 min of exposure to H_2O_2. The decrease in P_o occurred abruptly after a lag time that was [H_2O_2] dependent. With 8 mM H_2O_2, the lag time was ~10 min but was almost absent when 23 mM H_2O_2

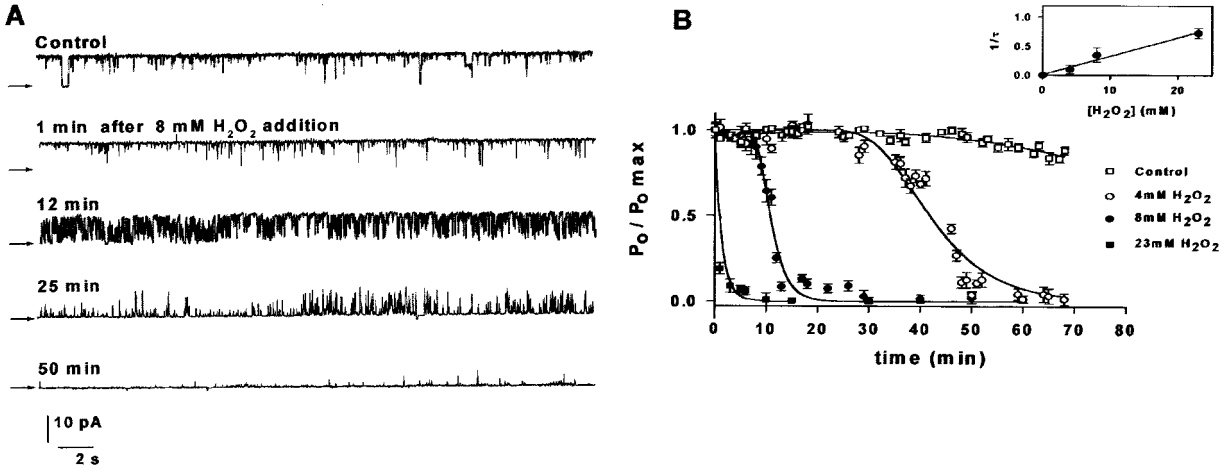

Fig. 2. H_2O_2 decreases the P_o of the Ca^{2+}-sensitive voltage-dependent K^+ ($K_{V,Ca}$) channel. *A*: single-channel current records in the absence (control) and in the presence of 8 mM internal H_2O_2 after 1, 12, 25, and 50 min of addition. Arrows indicate the closed state. *B*: time course of the $K_{V,Ca}$ channel P_o decreases after addition of 4 (○), 8 (●), and 23 mM H_2O_2 (■). □, Data taken in the absence of H_2O_2. Transmembrane potential was +60 mV. Data are presented as means ± SD for $n = 5$. Solid lines are fits to the data using *Eq. 4*. For 4 mM H_2O_2, $n = 103$ and $\tau = 8.35 \pm 0.13$ min; for 8 mM H_2O_2, $n = 103$ and $\tau = 2.15 \pm 0.30$ min. The data obtained using 23 mM H_2O_2 were fit to a single exponential with $\tau = 0.62 \pm 0.09$ min.

was added to the internal side. At this concentration, the P_o decreased more than 50% in ~2 min. When [H_2O_2] was 4 mM, the channel activity decreased after lag periods longer than 30 min (Fig. 2*B*).

After 30 min in the presence of 23 mM H_2O_2, the decrease in P_o could not be reversed either by extensive washing with an oxidant-free solution (Fig. 3, *A* and *D*) or by increasing [Ca^{2+}] in the internal side to 60 μM (Fig. 3, *B* and *E*). In the absence of H_2O_2 ($t = 0$, control), the P_o value was 0.879 ± 0.089 ($n = 4$), and after 30 min in the presence of 23 mM H_2O_2, the P_o value decreased to 0.065 ± 0.024 ($n = 4$). In 20 different single-channel membranes, the effect of H_2O_2 was irreversible when $P_o \leq 0.01$. $K_{V,Ca}$ channels that reach that low a P_o cannot recover with increasing internal [Ca^{2+}]. At a less dramatic decrease in P_o, the H_2O_2 increasing internal [Ca^{2+}] reversed effect. For example, after 4 min of the addition of 18 mM H_2O_2, the effect was reversed by increasing the [Ca^{2+}] to 200 μM in the internal side (Fig. 3, *C* and *F*). From these results it is apparent that the oxidizing reactions go through a series of reversible steps ending in one or more irreversible steps. According to the multiple-hit model, the initial hits would have the effect of increasing the energy that separate closed from open states shifting the P_o-voltage curve to the right. Control P_o can be recovered in this case by increasing the [Ca^{2+}] or voltage. However, when the channel-oxidizing reaction is complete, the channel enters in an absorbent quiescent state that cannot be reversed by an increase in [Ca^{2+}] or voltage.

Desferrioxamine and cysteine protect K^+ channel activity against ·OH. H_2O_2 in the presence of Fe(II) can generate ·OH via the Fenton reaction (28), where H_2O_2 is reduced according to the following scheme: $Fe^{2+} + H_2O_2 \rightarrow {\cdot}OH + Fe^{3+} + {}^{-}OH$. This reaction is a well-known source of ·OH, and there is evidence that the iron-mediated production of ·OH is an important source of lipid peroxidation and oxidation of amino acid residues in proteins (28).

To test whether the effect of H_2O_2 in the channel was mediated by ·OH generated from contaminant Fe^{2+} or

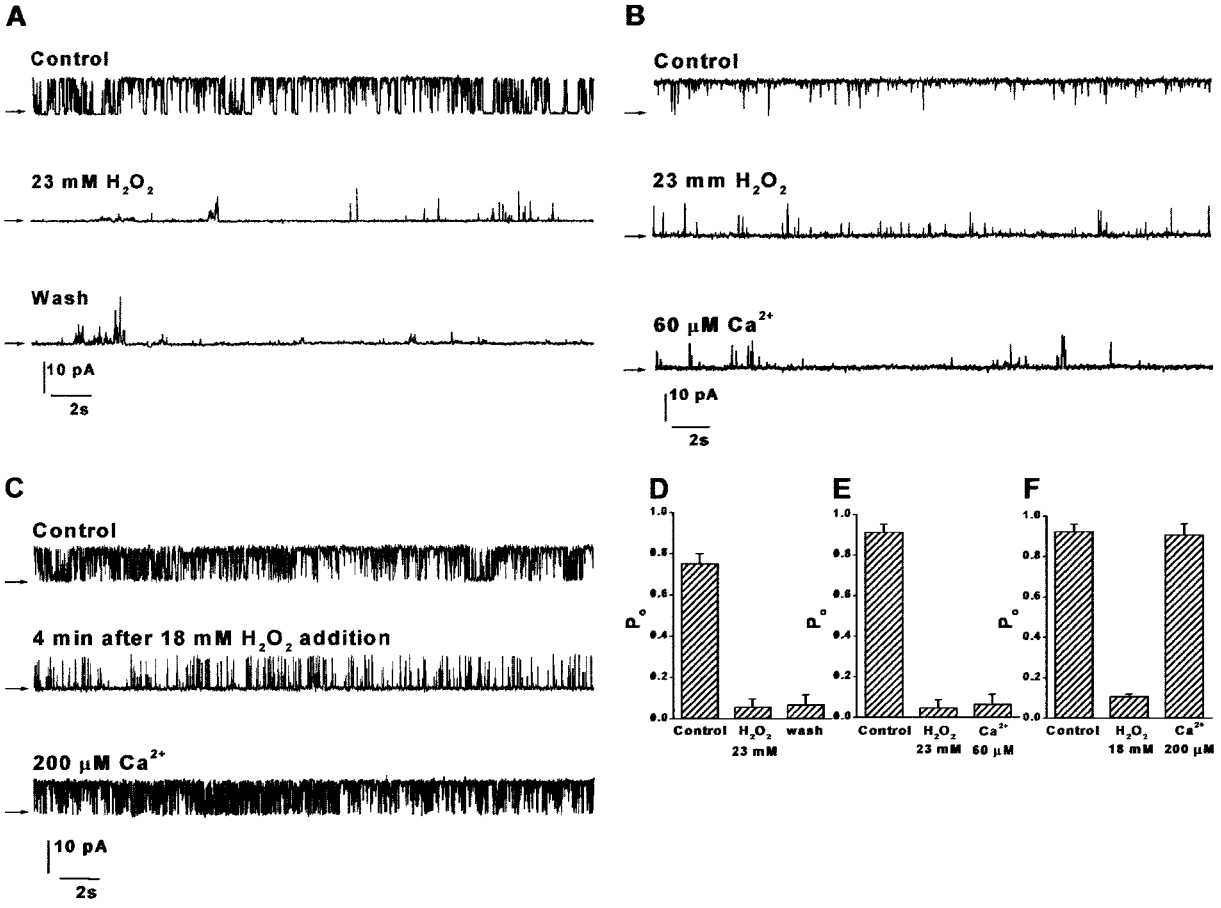

Fig. 3. Reversibility of the H_2O_2 effect on the $K_{V,Ca}$ channel. *A*: after a control period in the absence of the oxidizing agent (*top*), H_2O_2 was added to the internal side of the channel to a final concentration of 23 mM (*middle*). After 30 s in the presence of H_2O_2, P_o decreased to 0.105; after several minutes in the presence of H_2O_2, the internal compartment was perfused with 10 volumes of a H_2O_2-free solution (*bottom*). *B*: experiment done as in *A*, except that reversibility was tested by perfusing the internal compartment with a H_2O_2-free solution containing 60 μM Ca^{2+}. *C*: $K_{V,Ca}$ channel activity can be recovered if, after 18 mM H_2O_2 treatment, the internal compartment is perfused with a solution containing 200 μM of Ca^{2+}. The [Ca^{2+}] was 5 μM during the control period and after addition of H_2O_2. *D*, *E*: average from 4 different experiments under the conditions described in *A* and *B* (means ± SD), respectively. *F*: data from 5 experiments under the conditions described in *C* (means ± SD).

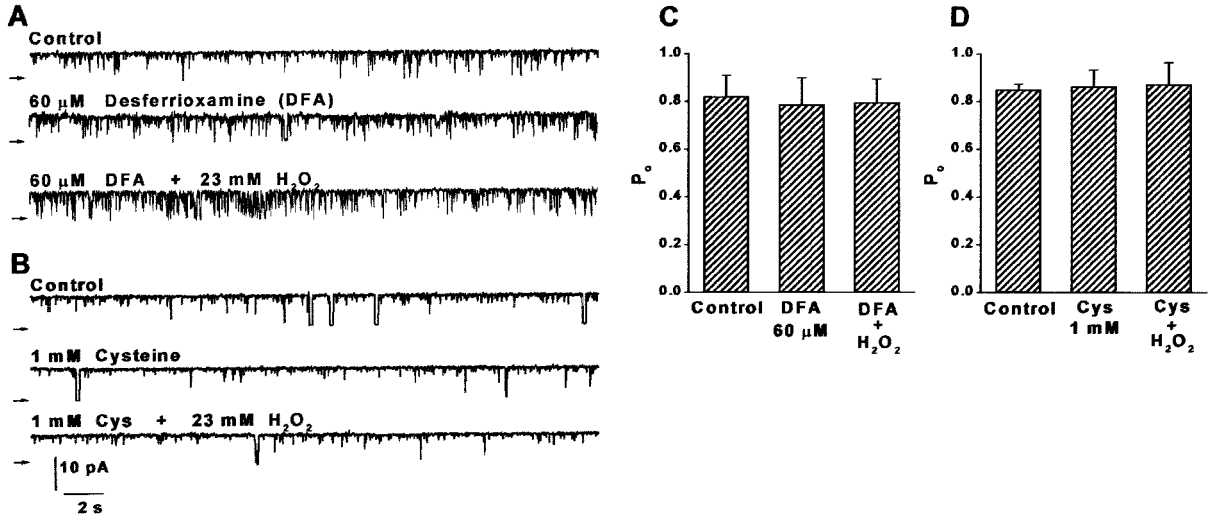

Fig. 4. Desferrioxamine (DFA) and cysteine (Cys) protect against the deleterious effect of H_2O_2. *A*: after a control period of 3 min, 60 μM DFA was added to the internal side of the bilayer. DFA protects against the effect of H_2O_2, as can be observed in the third single-channel record. *B*: Cys (1 mM) added before H_2O_2 (23 mM) protects from the decrease in P_o. *C*, *D*: average of 4 experiments (means ± SD) under the conditions described in *A* and *B*, respectively.

by the H_2O_2 itself, we added desferrioxamine or cysteine to the internal chamber. Desferrioxamine prevents ·OH formation, and cysteine is an efficient scavenger of ·OH. Desferrioxamine oxidizes Fe^{2+} to Fe^{3+} in the presence of O_2 and, if applied before H_2O_2 addition to the chamber, protects against the formation of ·OH via the Fenton reaction. Figure 4*A* shows that in the presence of 60 μM desferrioxamine in the cytoplasmic side of the channel, the addition of 23 mM H_2O_2 does not promote a rundown of P_o even after an exposure time of 25 min. Figure 4*C* shows the average of five experiments in a bar graph. On the other hand, cysteine (a reducing agent) acts as an electron donor from sulfhydryl groups. Figure 4*B* shows single-channel recordings in the presence of 1 mM cysteine in the internal side and the average of four experiments in a bar graph (Fig. 4*D*). Similar to what was observed for desferrioxamine, in the presence of cysteine, 23 mM H_2O_2 did not cause a reduction in the P_o even after 25 min of H_2O_2 exposure.

Effect of sulfhydryl groups reducing agents. Confirming previous reports (10, 38, 39), we found that channel activity in lipid bilayers was increased by exposure of the intracellular side to the sulfhydryl (SH) reducing agent DTT (2 mM; Fig. 5*A*). For this experiment, we chose channels with a low P_o at the calcium concentration used (~5 μM). Figure 5, *A* and *C*, shows that P_o increased 2.3-fold after we added 2 mM DTT (0.260 ± 0.096 to 0.608 ± 0.134, $n = 4$). After DTT addition, the increase in P_o took less than 30 s to reach a steady state and remained constant during usual recording times (15–30 min). Perfusion of the internal side with

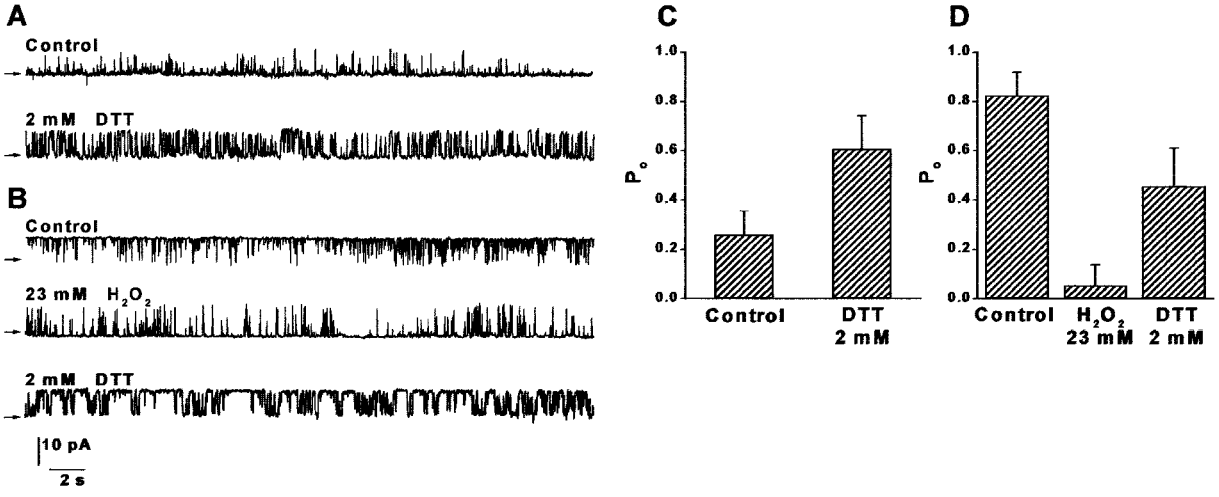

Fig. 5. Dithiothreitol (DTT) can partially recover the activity of H_2O_2-modified $K_{V,Ca}$ channels. *A*: channels having a P_o of ~0.3 at 5 μM Ca^{2+} were chosen; 2 mM DTT added to the internal side of the bilayer increased their P_o. *B*: the addition of 2 mM DTT partially recovers the activity of a H_2O_2-modified channel. *C*: the average increase in P_o was from 0.260 to 0.608, $n = 4$. *D*: average recovery for 4 experiments was 55% of control values.

a DTT-free solution did not reverse the DTT effect. The effect of 23 mM H_2O_2 on channel activity was partially reversed by adding 2 mM DTT after perfusing the intracellular side with about ten times the volume of the internal compartment with a H_2O_2-free buffer (Fig. 5, *B* and *D*). P_o values were: control P_o, 0.896 ± 0.124; P_o in the presence of 23 mM H_2O_2, 0.054 ± 0.006; and P_o in the presence of 2 mM DTT, 0.511 ± 0.156.

Modification of SH groups by DTNB. To determine if SH residues were involved in channel modulation by redox agents, we used DTNB. DTNB is a hydrophilic oxidative reagent that attacks specifically SH groups in proteins in a reaction that involves a thiol-disulfide exchange mechanism. Figure 6*A* shows the effect of 2 mM internal DTNB on channel activity. P_o decreased 17-fold (P_o = 0.052 ± 0.007) compared with control (P_o = 0.889 ± 0.103). Channel activity was not restored by withdrawal of DTNB from the internal side of the channel, suggesting a covalent modification. However, channel activity was almost fully restored by application of 2 mM DTT to the internal side (Fig. 6, *A* and *B*). On the average, in the presence of 2 mM internal DTT, P_o increased to 0.76 ± 0.13 of the initial control value. This observation strongly suggests that the observed inhibitory effect of DTNB is specifically related to the oxidation of SH groups.

Effect of H_2O_2 on the macroscopic current induced by hSlo channels. Figure 7 shows the effect of H_2O_2 on the macroscopic $K_{v,Ca}$ currents expressed in *X. laevis* oocytes. The addition of H_2O_2 to the external side (in the pipette) caused a decrease of ~5% of the current after 3–5 min of seal formation. No further changes were observed thereafter (Fig. 7*A*). Incubation of an inside-out patch for 30 min in the presence of 8 mM H_2O_2 reduced the macroscopic current by 60% (Fig. 7*B*). After 1 h, the current decreased further to about 20% of the control value. Under these conditions, we obtained data by directly plotting the peak tail current amplitude at a constant postpulse potential (−60 mV) and as a function of the test prepulse potential in symmetrical 110 mM K^+ (Fig. 7*C*). Note that H_2O_2 addition at the internal side induces a gradual shift of the tail conductance vs. voltage curves, with a clear decrease in the maximum conductance.

DiChiara and Reinhart (10) reported a spontaneous decline in the macroscopic K^+ current induced by h*Slo* channels after patch excision that was reversed by 1 mM DTT. We also found a current rundown after patch excision, but it was much less pronounced than the one reported by DiChiara and Reinhart. H*Slo* macroscopic conductance decreased by about 8% 5 min after patch excision and then remained constant for periods as long as 1 h (data not shown). The reason for the difference between our results and those DiChiara and Reinhart (10) is unclear. To avoid an overestimation of the channel inhibition induced by H_2O_2 due to rundown, we added H_2O_2 to the internal solution 5–10 min after patch excision. $I_{tail}(V)$ is given by the relationship

$$I_{tail}(V) = NiP_o(V) \quad (2)$$

or

$$G_{tail}(V) = NgP_o(V) \quad (3)$$

where i is current amplitude of the single channel, g is unitary conductance, N the number of channels, and $P_o(V)$ the voltage-dependent open probability. Single-channel current measurements showed that g is constant; therefore, the fact that G_{tail} decreases may indicate a reduction in the number of channels and/or a decrease in P_o (see *Eq. 3*). To obtain a proper determination of the P_o^{max} behavior during H_2O_2 exposure, we used the nonstationary fluctuation analysis (14, 31–33). Figure 8, *A*, *D*, and *G*, shows the time course of average current for a +120-mV pulse at 0, 10, and 30 min of H_2O_2 exposure. The noise fluctuations in Fig. 8, *B*, *E*, and *H*, have a biphasic time course that is a reflection of the channel P_o during the activation of the ionic current. The variance vs. current plots in Fig. 8, *C* and *F*, were fitted to *Eq. 1*. The fitted parameters were

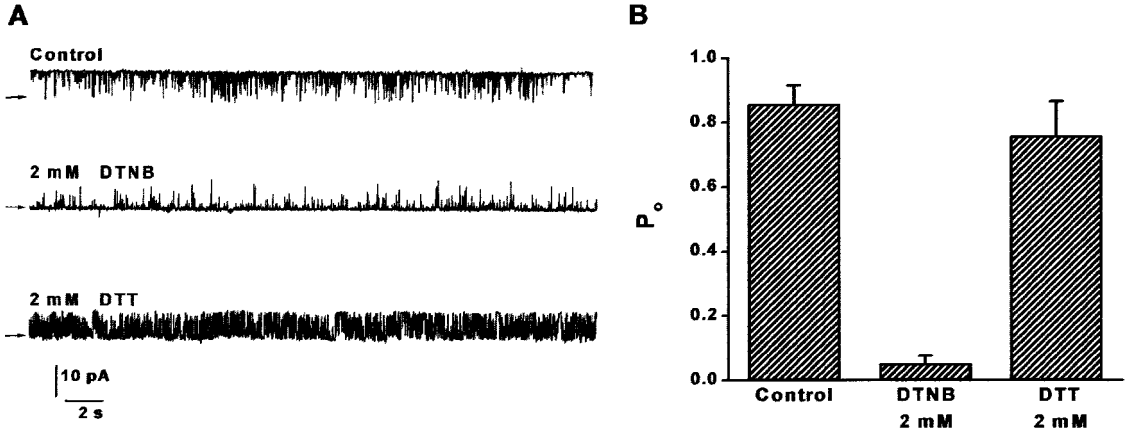

Fig. 6. DTT recovers the activity of 5,5′-dithio-bis-(2-nitrobenzoic acid) (DTNB)-modified channels. *A*: currents recorded in control conditions (*top* trace), after 2 mM DTNB was added to the internal side of the channel (*middle* trace), and after removing DTNB by washing and adding 2 mM DTT (*bottom* trace). *B*: average of 4 different experiments. Control P_o values decreased from 0.889 to 0.052 with DTNB. Addition of 2 mM DTT to the cytoplasmic side of the channel increased P_o to 0.758. [Ca^{2+}] was 5 μM.

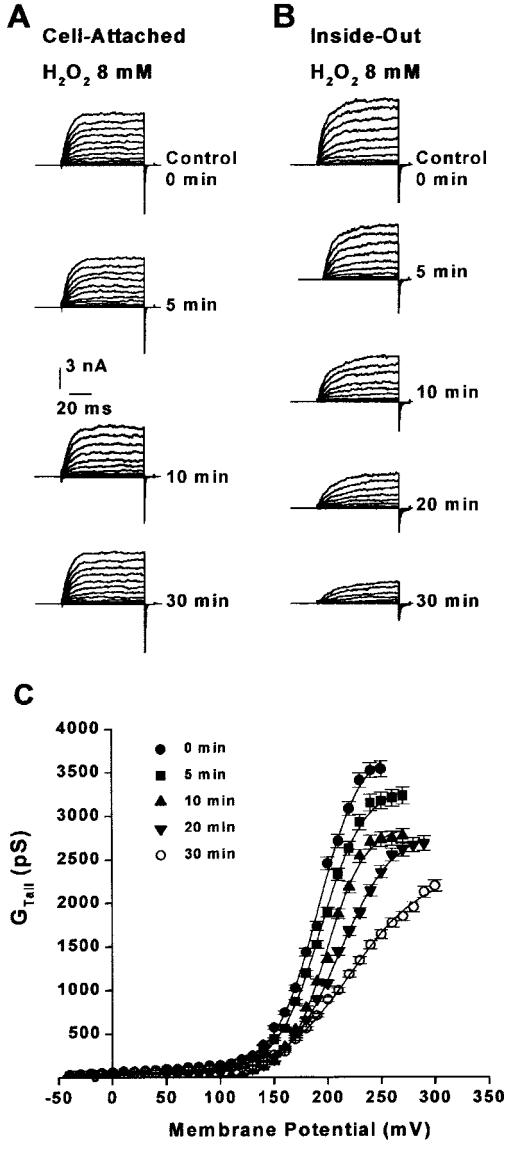

Fig. 7. H_2O_2 inhibits $K_{V,Ca}$ channel steady-state currents when added to the intracellular side. *A*: macroscopic currents in the cell-attached configuration were recorded in the range −150 to 140 mV. H_2O_2 (8 mM) was added in the pipette. *B*: $K_{V,Ca}$ current recorded in an inside-out patch was recorded in the range −50 to 140 mV at 10-mV increments. H_2O_2 (8 mM) was added in the bath. Internal $[Ca^{2+}]$ = 56 nM. *C*: conductance (G_{tail}) vs. voltage curves for the traces shown in *B*. Data were obtained measuring the peak amplitude of the tail currents after repolarization to −60 mV in the range −40 mV to 250–300 mV. Each point is the average of 5 patches in the inside-out configuration. The experimental data were fitted to a Boltzmann equation of the form $G_{tail} = G_{max}/\{1 + \exp[(V_{1/2} - V)/k]\}$ where V is the applied voltage, $V_{½}$ is the half-activation voltage, and k the slope of the G_{tail} vs. voltage curve. G_{max} was 3,500, 3,100, 2,750, 2,600, and 2,150 pS for the G_{tail} vs. voltage curves taken at 0, 5, 10, 20, and 30 min, respectively.

i = 37.0 ± 2.3 pA and N = 156 ± 15 channels in control conditions. P_o^{max}, obtained using the relation $P_o^{max} = I_{max}/iN$, was 0.63. Nonstationary fluctuation analysis was done after 10 min of H_2O_2 reaction (Fig. 8, *D–F*). During this period, we found a decrease in the number of channels by about one-third with respect to the control value. The fitting parameters are i = 34.6 ± 2.7 pA, N = 111 ± 8 channels, and P_o = 0.6. After 30 min of H_2O_2 exposure, the variance vs. current plot in Fig. 8*I* does not reach a maximum, indicating a clear decrease in P_o. Because the variance vs. current plot does not reach a maximum, it is not possible to fit the data to *Eq. 1*. These experiments indicate that H_2O_2 promotes both a decrease in the number of active channels and in P_o.

Effect of calcium after treatment with H_2O_2 on hSlo channel current. At low $[Ca^{2+}]$, the addition of 18 mM H_2O_2 produces a decrease in macroscopic current after 20 min of exposure (Fig. 9*A*). This effect was reversed by increasing the internal $[Ca^{2+}]$ to 100 μM. This effect was similar to that observed in single-channel experiments (Fig. 3, *C* and *F*). H_2O_2 addition at the internal side induces a shift of the tail conductance vs. voltage curves, with a clear decrease in the maximum conductance. As can be observed in Fig. 9*B*, the effect of the oxidant can be fully reversed by perfusing the internal side of the channel with a H_2O_2-free solution containing 100 μM Ca^{2+}. In the presence of high Ca^{2+} (100 μM), the addition of 18 mM H_2O_2 does not produce a decrease in the macroscopic current after 20 min of exposure (Fig. 10, *A* and *B*).

DISCUSSION

The interest in H_2O_2 as a biologically active oxygen-derived intermediate is evident, because it is associated to a series of alterations and effects in many

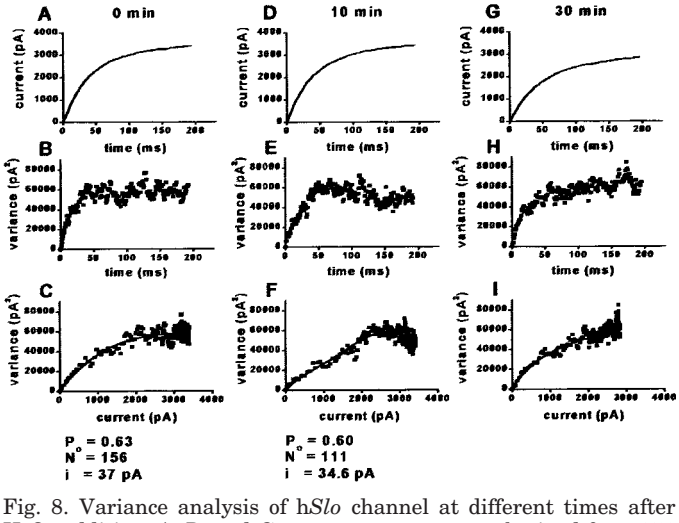

Fig. 8. Variance analysis of h*Slo* channel at different times after H_2O_2 addition. *A*, *D*, and *G*: mean current traces obtained from 256 traces recorded with the patch technique from a holding potential of 0 mV to a test pulse potential 120 mV at 0, 10, and 30 min after addition of 8 mM H_2O_2 to the internal side, respectively. *B*, *E*, and *H*: time course of the variance. *C*, *F*, and *I*: variance (σ^2) vs. mean current [$I(t)$] fitted to the function: $\sigma^2 = iI(t) - I(t)^2/N$ (solid line), where N is the number of channels and i the unitary current. At t = 0 min, maximum P_o was 0.63, i = 37.0 ± 2.3 pA, and N was 155,700 ± 15; after 10 min of H_2O_2 exposure, P_o = 0.60, i = 34.6 ± 2.7 pA, and N = 111,000 ± 8. After 30 min of H_2O_2 exposure, a clear maximum cannot be observed, which implies that $P_o \leq 0.5$. i was calculated from the slope of the σ^2 vs. $I(t)$ curve. Internal $[Ca^{2+}]$ was 728 nM, and V is 120 mV.

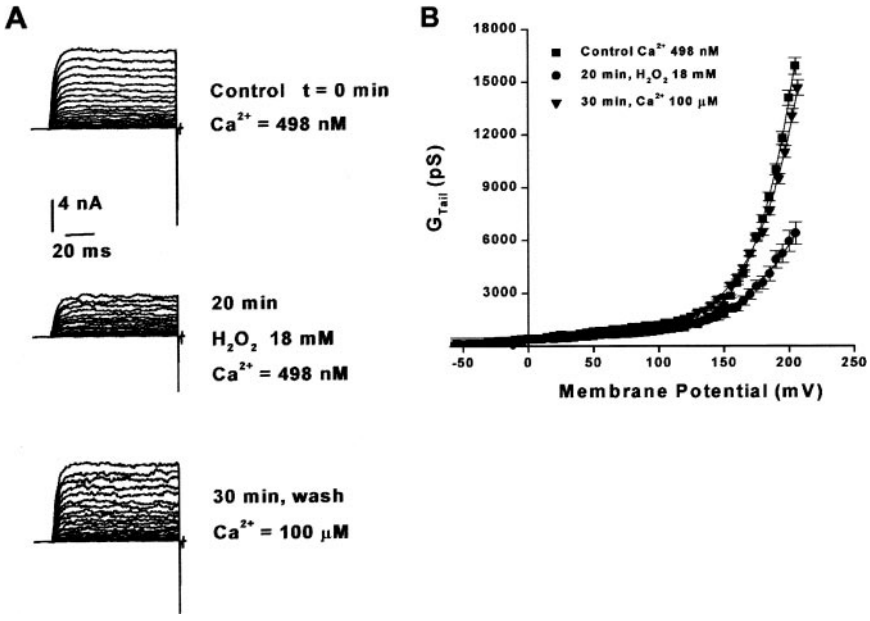

Fig. 9. High $[Ca^{2+}]$ recovers the activity of H_2O_2-modified channels. *A*: macroscopic currents were recorded using the patch-clamp technique in the inside-out configuration. The condition is the same as that in Fig. 7, but internal $[Ca^{2+}]$ = 498 nM and $[H_2O_2]$ = 18 mM. *B*: G_{tail} vs. voltage curves for the traces shown in A. Each point is the average of 5 patches in the inside-out configuration. G_{max} was 15,500, 6,000, and 14,800 pS for the G_{tail} vs. voltage curves taken at 0, 20, and 30 min, respectively. $[Ca^{2+}]$ at t = 30 min was 100 μM.

different types of cells. H_2O_2 is not by itself reactive enough to oxidize organic molecules in an aqueous environment. Nevertheless, H_2O_2 has the ability to generate highly reactive hydroxyl free radicals through its interaction with redox-active transitional metals (2). Hydroxyls result from the decomposition of H_2O_2 via the Fenton reaction and by interaction of superoxide with H_2O_2 through the Haber-Weiss reaction (41). The biological importance of H_2O_2 stems from its participation in the production of more reactive chemical species such as ·OH, and its role as a source of free radicals has been emphasized rather than its chemical reactivity. ·OH is considered one of the most potent oxidants encountered in biological systems. However, because of its extremely short half-life, it is effective only near the locus of its production. The diffusion capability of ·OH is restricted to only about two molecular diameters before it reacts with water (41). Highly reactive ·OH readily react with a variety of molecules, such as amino acids and lipids, by removing hydrogen or by addition to unsaturated bonds (28). The lag time and its dependence on $[H_2O_2]$ can be explained using a simple model in which n number of successful and independent hits of the H_2O_2 with different amino acid residues are necessary to "kill" a channel. A successful hit is described by the irreversible reaction

$$X \xrightarrow{k_1[H_2O_2]} X_{mod}$$

where X_{mod} is the residue modified by the hydrogen peroxide and k_1 the second-order rate constant describ-

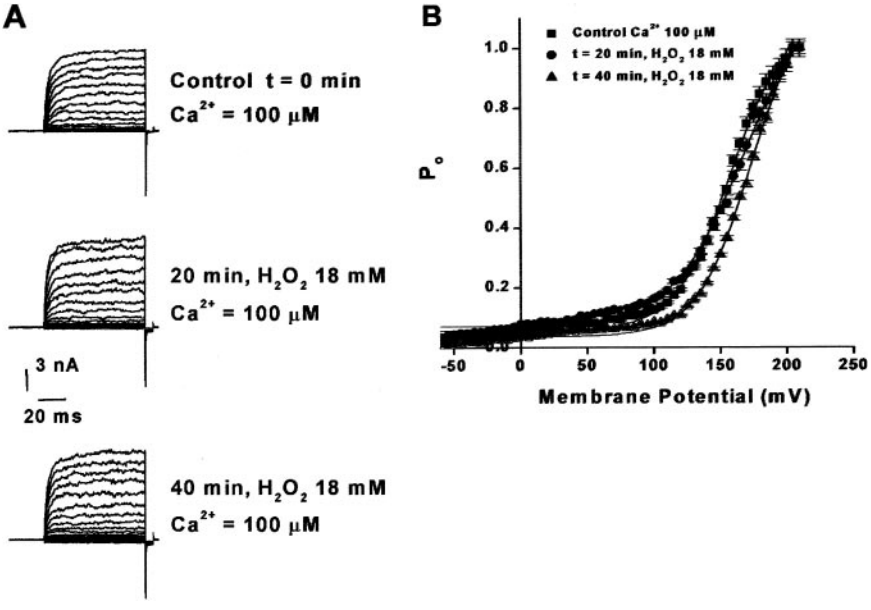

Fig. 10. High $[Ca^{2+}]$ supports activity of $K_{V,Ca}$ against the deleterious effect of H_2O_2. *A*: macroscopic current was recorded in the inside-out configuration under the same conditions described for Fig. 7. *B*: relative conductance ($G/G_{max} = P_o$) vs. voltage curves. In the control condition at t = 0, $[Ca^{2+}]$ was 100 μM (■). ●, After 20 min of exposure to 18 mM H_2O_2 addition. ▲, After 40 min of exposure to 18 mM H_2O_2. The fit curve was the same that Fig. 7.

ing the its chemical modification. In this model, the time dependence of the probability of opening, $P_o(t)$, is given by the expression

$$P_o(t) = 1 - [1 - \exp(-t/\tau)]^n \quad (4)$$

where $\tau = 1/k_1[H_2O_2]$ is the time constant. The best fit to the data of Fig. 2*B* (4 and 8 H_2O_2 mM) was obtained with $n = 103$. This number is very large indeed and can be explained on the basis of the large number of cysteine residues (108) present in the carboxy terminal of the $K_{V,Ca}$ channel. Below we show that cysteine residues are the main target of the oxidant agent, although it is likely that methionine or tryptophan residues are also oxidized.[1] Hovewer, other mechanisms are possible, and the interpretation of the n should be taken cautiously. The model proposed demands that the value of $1/\tau$ must be directly proportional to the $[H_2O_2]$. The inset of Fig. 2*B* shows that the $1/\tau - [H_2O_2]$ data are well described by a straight line with a second-order rate constant $k_1 = 0.56\ s^{-1}M^{-1}$. The value obtained for k_1 indicates that the oxidation is extremely slow indeed, considering that the forward rate constant in a diffusion-limited reaction is of the order of $10^8 - 10^9\ s^{-1}M^{-1}$. The very short half-life of the ·OH can explain the low forward rate constant, k_1, for the channel oxidizing reaction (Fig. 2*B*), obtained using the multiple-hit model because the effective [·OH] at the target sites in the protein would be low. We note here that the oxidizing reaction is a multistep process in which ·OH are formed via the Fenton reaction, reacting afterwards with, for example, an −SH group at a diffusion-controlled rate to form sulfinic or sulfonic acid derivatives (see, e.g., 18, 36). Therefore, the effective [·OH] should be in the nanomolar range to explain the low reaction rate found in Fig. 2*B*.

In the present work we found that adding H_2O_2 to the cytoplasmic aspect of the $K_{V,Ca}$ channel produces a decrease in its P_o (Fig. 2). This effect was not reversed by washing or after increasing $[Ca^{2+}]$ to 60 μM (Fig. 3*B*). Therefore, H_2O_2 could be involved in redox reactions with some vulnerable amino acid residues (28). The protective effect showed by desferrioxamine and cysteine before treatment with 23 mM H_2O_2 (Fig. 4) implies that the decrease in P_o is mediated by the ·OH generated by the Fenton reaction.

Of course, it is possible that the oxidant agent affects other components associated to the membrane or to the channel; for example, the target of the oxidizing agent could be an auxiliary β-subunit or some membrane-bound enzyme able to promote channel phosphorylation. We think that the bilayer experiments argue against that possibility, because the skeletal muscle preparation does not contain β-subunits and we are working in the absence of second messengers such as ATP or cAMP. In what follows, we assume that the primary target of the ·OH is the channel-forming protein.

The decrease in the $K_{V,Ca}$ channel activity by addition of H_2O_2 to the intracellular side is highly dependent on the oxidant concentration. Low $[H_2O_2]$ (8 mM) does not affect the P_o of $K_{V,Ca}$ channels in the first 8 min of a reaction. Afterwards, and in a very short time span, P_o values change drastically. Based on the effect of desferrioxamine, the reduction in P_o can be attributed to the oxidizing action of the ·OH on free SH residues of cysteines associated with the opening of the $K_{V,Ca}$ channel. The differences in the effect of the H_2O_2 when it is added to the intracellular or extracellular side imply different access to essential targets. In particular, oxidation of free SH residues of cysteines, present in greater proportion at the intracellular side (27 amino acid residues per subunit), could explain the observed difference. Twenty-four of these residues occur in transmembrane or intracellular domains and are largely concentrated in the carboxy terminus of the h*Slo* protein. We think that the external cysteines (C14, C141, and C277) do not play an important functional role in determining P_o, because their replacement by serine produces channels indistinguishable from the wild-type in terms of voltage-Ca^{2+} dependence and H_2O_2 sensitivity (data not shown).

To determine whether the P_o decrease of the $K_{V,Ca}$ channel by ·OH could be attributed to the oxidation of free SH residues of cysteine, the effect of H_2O_2 was compared with that of DTNB. This is a hydrophilic agent specific for the oxidation of free SH groups in proteins. The presence of 2 mM DTNB decreased the P_o value to an extent similar to that observed with H_2O_2. This effect was reversed by addition of 2 mM DTT (Fig. 6*A*). On the other hand, the addition of 2 mM DTT to a channel previously treated with H_2O_2 only produces a partial recovery in the P_o (Fig. 5*B*). These results would indicate that $K_{V,Ca}$ channel of rat skeletal muscle can be regulated by compounds that alter the redox states of sulfhydryl groups. Similar behavior was described for a smooth muscle $K_{V,Ca}$ channel (38, 39) and a voltage-insensitive K(Ca^{2+}) channel of intermediate conductance present in bovine aortic endothelial cells (5). Cai and Sauvé (5) show that the oxidative effects of H_2O_2 were observed at H_2O_2 concentrations ranging from 0.5 to 10 mM. The oxidative effect of H_2O_2 was similar to hydrophilic oxidative reagents such as DTNB. The difference observed between the $K_{V,Ca}$ channel activity recovery by DTT in pretreated samples with H_2O_2 (Fig. 5*C*) (recovery 57%) and that with DTNB (Fig. 6*A*) (recovery 85%) indicates that the ·OH could have a more generalized oxidative effect than DTNB. Besides cysteines, other amino acids such as tryptophan and/or methionine can be the target of the ·OH (7, 23, 28).

We note here that the addition of H_2O_2 in presence of high calcium (Fig. 9) does not produce a macroscopic conductance decrease after 20 min of exposure. In this condition, high internal $[Ca^{2+}]$ would act as a protective Ca^{2+} agent for the different sensitive groups exposed in the carboxy-terminal region, particularly at

[1] We show below that ·OH via the Fenton reaction mediate the H_2O_2 effect. This fact will not affect the conclusion extracted using the model used to fit the P_o-time data since the [·OH] is directly proportional to the $[H_2O_2]$.

calcium binding sites (29). These experimental facts could be important, due to the fact that the intracellular Ca^{2+} is modulating and potentially protecting groups that can be oxidized and are associated to the opening and closing of the $K_{V,Ca}$ channel.

Oxidation effects depend on the type of K^+ channels. The effect of ROS on the $K_{V,Ca}$ channel differs from that reported for voltage-dependent K^+ or the human ether-à-gogo-related gene (HERG) channels. For example, *t*-butyl hydroperoxide reversibly increases the activity of both Kv1.4 and Kv3.4. This effect was attributed to an attenuation or removal of the fast inactivation processes (11). Enhancement of ROS production induced by the perfusion with Fe^{2+} and ascorbic acid caused an increase in HERG outward K^+ currents (34). On the other hand, a decrease in ROS levels achieved by perfusion with ROS scavengers inhibited the resting outward currents induced by HERG channels and prevented their increase induced by ROS. Rose bengal (generator of singlet oxygen, $^1O_2$) produced a decrease of channel activity in the case of Shaker, Kv1.3, Kv1.4, Kv1.5, and Kv3.4 channels expressed in *Xenopus* oocytes. Duprat et al. (11) argued that these observations might be important in disease states. Kv1.4 and Kv1.5 are fast inactivating channels expressed in cardiac cells, and their inhibition by ROS can contribute to the major electrophysiological disorders that occur during reperfusion-induced arrhythmias after ischemia and during heart failure induced by chronic pressure overload (3). Evidence of a direct effect of H_2O_2 on ATP-sensitive K^+ (K_{ATP}) channels was inferred from studies where ROS effects were examined on excised membrane patches. Ichinari et al. (16) observed a dose-dependent H_2O_2-induced increase in P_o of the K_{ATP} channel. H_2O_2-induced irreversible inhibition of the activity of K_{ATP} channel in skeletal muscle has been attributed to inhibition via oxidation of SH groups (40). On the other hand, sarcoplasmic reticulum Ca^{2+} release channel (ryanodine receptor) is differentially affected by different ROS. Singlet oxygen causes an irreversible damage of the ryanodine from cardiac muscle after a brief transient period of activation (15). However, 5 mM H_2O_2 activates the same channel even at 0.45 nM cytosolic calcium, a condition in which the channel is normally silent. The activation occurs abruptly after a lag period of a few minutes (4). The activating effect of H_2O_2 has also been found for the ryanodine receptor from skeletal muscle channel of the rabbit and frog (12, 26). The rabbit channel is somewhat more sensitive; it becomes activated at 0.1 mM, and in this preparation 1–3 mM H_2O_2 inhibit channel activity (12).

The range of $[H_2O_2]$ used by different authors varies from 0.1 to 50 mM (19). The exact physiologically significant concentration is not clearly defined and may depend on the cellular type. For example, the potassium channel KShIIID.1 expressed in *Xenopus* oocytes is sensitive to 10 μM H_2O_2. The current through this particular channel is very similar to the currents sensitive to the arterial O_2 pressure found in chemoreceptor neurons, where 10 μM H_2O_2 does modify neuronal activity (37). The intracellular $[H_2O_2]$ reached during exercise in skeletal muscle have not been determined, but because H_2O_2 effects develop progressively after repeated tetanic contractions, the accumulation of H_2O_2 could affect skeletal muscle channels.

Recently, Tang et al. (35) found that at the intracellular side, methionine oxidation by chloramine-T produces an increase of the P_o mediated by an increase in voltage-dependent opening transitions and a slowing down of the closing transition rate.

They observed that the stimulatory effect of chloramine-T is maintained in the cysteine-less mutant channel (35). Our results indicate that the ·OH had a wide oxidative effect, which does not contradict their results.

We thank Dr. Eduardo Rosenmann for critical reading of the manuscript, Dr. Osvaldo Alvarez for suggesting to us the multiple-hit model, and Luisa Soto for excellent technical assistance. Drs. Enrico Stefani and Ning Zhu kindly shared with us the external cysteine-less mutant.

This work was supported by Chilean Fondo Nacional de Investigacion Científica y Tecnológica Grants 398-0005 (M. Soto), 100-0890 (R. Latorre), and 198-1053 (C. Vergara); by Cátedra Presidencial en Ciencia (R. Latorre and E. Lissi); and the Human Frontier in Science Program (R. Latorre). Centro de Estudios Científicos is a Millenium Science Institute.

REFERENCES

1. **Anwer K, Oberti C, Pérez G, Pérez-Reyes N, McDougall J, Sanborn B, Stefani E, and Toro L.** Calcium-activated K^+ channels as modulators of human myometrial contractile activity. *Am J Physiol Cell Physiol* 265: C976–C985, 1993.
2. **Aruoma O, Halliwell B, Gajewski E, and Dizdaroglu M.** Copper-iron dependent damage to the bases in DNA in the presence of hydrogen peroxide. *Biochem J* 273: 2601–2604, 1991.
3. **Bing O.** Hypothesis: apoptosis may be a mechanism for the transition to heart failure with chronic pressure overload. *J Mol Cell Cardiol* 26: 943–948, 1994.
4. **Boraso A and Williams A.** Modification of the gating of the cardiac sarcoplasmic reticulum Ca^{2+}-release channel by H_2O_2 and dithiothreitol. *Am J Physiol Heart Circ Physiol* 267: H1010–H1016, 1994.
5. **Cai S and Sauvé R.** Thiol-modifying agents on a K(Ca^{2+}) channel of intermediate conductance in bovine aortic endothelial cells. *J Membr Biol* 158: 147–158, 1997.
6. **Cecchi X, Wolff D, Alvarez O, and Latorre R.** Mechanisms of Cs^{2+} blockade in Ca^{2+}-activated K^+ channels from smooth muscle. *Biophys J* 52: 707–716, 1987.
7. **Ciorba M, Heinemann S, Weissbach H, Brot N, and Hoshi T.** Modulation of potassium channel function by methionine oxidation and reduction. *Proc Natl Acad Sci USA* 94: 9932–9937, 1997.
8. **Davies K, Quintanilha A, Brooks G, and Parker L.** Free radicals and tissue damage produced by exercise. *Biochem Biophys Res Commun* 107: 1198–1205, 1982.
9. **Díaz F, Wallner D, Stefani E, Toro L, and Latorre R.** Interaction of internal Ba^{2+} with a cloned Ca^{2+}-dependent K^+(h*Slo*) channel from smooth musculature. *J Gen Physiol* 107: 339–407, 1996.
10. **DiChiara TJ and Reinhart PH.** Redox modulation of h*Slo* Ca^{2+}-activated K^+ channels. *J Neurosci* 17: 4942–4955, 1997.
11. **Duprat F, Guillemare E, Romey G, Fink M, Lesage F, Lazdunski M, and Honore E.** Susceptibility of cloned K^+ channels to reactive oxygen species. *Proc Natl Acad Sci USA* 92: 11796–11800, 1995.
12. **Favero T, Zable A, and Abramson J.** Hydrogen peroxide stimulates the Ca^{2+} release channel from skeletal muscle sarcoplasmic reticulum. *J Biol Chem* 270: 25557–25563, 1995.

13. **Finkel T and Holbrook NJ.** Oxidants, oxidative stress and the biology of ageing. *Nature* 408: 239–247, 2000.
14. **González C, Rosenman E, Bezanilla F, Alvarez O, and Latorre R.** Modulation of the Shaker K^+ channel gating kinetics by the S3–S4 linker. *J Gen Physiol* 15: 193–207, 2000.
15. **Holmberg SR, Cumming DV, Kusama Y, Hearse DJ, Poole-Wilson PA, Shattock MJ, and Williams AJ.** Reactive oxygen species modify the structure and function of the cardiac sarcoplasmic reticulum calcium-release channel. *C R Seances Soc Biol Fil* 2: 19–25, 1991.
16. **Ichinari K, Kakei M, Matsuoka T, Nakashima H, and Tanaka H.** Direct activation of the ATP-sensitive potassium channel by oxygen free radicals in guinea-pig ventricular cells: its potentiation by MgADP. *J Mol Cell Cardiol* 28: 1867–1877, 1996.
17. **Jagger J, Porter V, Lederer W, and Nelson M.** Calcium sparks in smooth muscle. *Am J Physiol Cell Physiol* 278: C235–C256, 2000.
18. **Khan AU and Kasha M.** Singlet molecular oxygen in the Haber-Weiss reaction. *Proc Natl Acad Sci USA* 91: 12365–12367, 1994.
19. **Kourie J.** Interaction of reactive oxygen species with ion transport mechanisms. *Am J Physiol Cell Physiol* 275: C1–C24, 1998.
20. **Latorre R, Oberhauser A, Labarca P, and Alvarez O.** Varieties of calcium-activated potassium channels. *Annu Rev Physiol* 51: 385–399, 1989.
21. **Latorre R, Vergara C, Álvarez O, Stefani E, and Toro L.** Voltage-gated calcium-modulated potassium channels of large unitary conductance: structure, diversity, and pharmacology. In: *Pharmacology of Ionic Channel Function*, edited by Endo M, Kurachi Y, and Mishina M. Berlin: Springer-Verlag, 2000, p. 197–223.
22. **Latorre R, Vergara C, and Hidalgo C.** Reconstitution in planar lipid bilayers of a Ca^{2+}-activated K^+ channel from transverse tubule membranes isolated from rabbit skeletal muscle. *Proc Natl Acad Sci USA* 79: 805–809, 1982.
23. **Lin C and Chen T.** Cysteine modification of a putative pore residue in ClC-0. Implication for the pore stoichiometry of ClC chloride channels. *J Gen Physiol* 116: 535–546, 2000.
24. **Nelson M, Cheng H, Rubart M, Santana L, Bonev A, Knot H, and Lederer W.** Relaxation of arterial smooth muscle by calcium sparks. *Science* 270: 633–637, 1995.
25. **Neyton J.** Ba^{2+} chelator suppresses long events in fully activated high-conductance Ca^{2+}-dependent K^+ channels. *Biophys J* 71: 220–226, 1996.
26. **Oba T, Koshita M, and Yamaguchi M.** H_2O_2 modulates twitch tension and increases P_o of Ca^{2+} release channel in frog skeletal muscle. *Am J Physiol Cell Physiol* 271: C810–C818, 1996.
27. **Phung C, Ezieme J, and Turrens J.** Hydrogen peroxide metabolism in skeletal muscle mitochondria. *Arch Biochem Biophys* 315: 479–482, 1994.
28. **Rice-Evans C, Diplock A, and Symons M.** Mechanisms of radical production. In: *Techniques in Free Radicals Research*, edited by Burdon R and van Knippenberg P. Amsterdam: Elsevier, 1991, p. 33–50.
29. **Schreiber M and Salkoff L.** A novel calcium sensing domain in the BK channel. *Biophys J* 73: 1355–1363, 1997.
30. **Sen C, Kolosova I, Hanninen O, and Orlov S.** Inward potassium transport systems in skeletal muscle derived cells are highly sensitive to oxidant exposure. *Free Radic Biol Med* 18: 795–800, 1995.
31. **Sigworth FJ.** The variance of sodium current fluctuations at the node of Ranvier. *J Physiol (Lond)* 307: 97–129, 1980.
32. **Sigworth FJ.** Covariance of nonstationary sodium current fluctuations at the node of Ranvier. *Biophys J* 34: 111–133, 1981.
33. **Stefani E, Ottolia M, Noceti F, Olcese R, Wallner M, Latorre R, and Toro L.** Voltage-controlled gating in large conductance Ca^{2+} sensitive K^+ channel (h*Slo*). *Proc Natl Acad Sci USA* 94: 5427–5431, 1997.
34. **Taglialatela M, Castaldo P, Iossa S, Pannaccione A, Fresi A, Ficker E, and Annunziato L.** Regulation of the human ether-a-gogo related gene (HERG) K^+ channels by reactive oxygen species. *Proc Natl Acad Sci USA* 94: 11698–11703, 1997.
35. **Tang X, Daggett H, Hanner M, García M, McMannus O, Brot N, Weissbach H, Heinemann S, and Hoshi T.** Oxidative regulation of large conductance calcium-activated potassium channels. *J Gen Physiol* 117: 253–274, 2001.
36. **Thannickal VJ and Fanburg BL.** Reactive oxygen species in cell signaling. *Am J Physiol Lung Cell Mol Physiol* 279: L1005–L1028, 2000.
37. **Vega-Saenz de Miera E and Rudy B.** Modulation of K^+ channels by hydrogen peroxide. *Biochem Biophys Res Commun* 186: 1681–1687, 1992.
38. **Wang Z and Kotlikoff M.** Regulation of Ca^{2+}-activated K^+ channel gating by sulfhydryl redox agents (Abstract). *Biophys J* 70: A401, 1996.
39. **Wang Z, Nara M, Wang Y, and Kotlikoff M.** Redox regulation of large conductance Ca^{2+}-activated K^+ channels in smooth muscle cells. *J Gen Physiol* 110: 35–44, 1997.
40. **Weik R and Neumcke B.** ATP-sensitive potassium channels in adult mouse skeletal muscle: characterization of the ATP-binding site. *J Membr Biol* 110: 217–226, 1989.
41. **Yu B.** Cellular defenses against damage from reactive oxygen species. *Physiol Rev* 74: 139–162, 1994.